Electronic Supplementary Information for

Controllable and facile preparation of Co_9S_8-Ni_3S_2 heterostructures embedded in N,S,O-*tri*-doped carbon for electrocatalytic oxidation of 5-hydroxymethylfurfural

Yibin Zhang,[a] Zhimin Xue,[a]* Xinhui Zhao,[b] Baolong Zhang[b] and Tiancheng Mu[b]*

[a]Beijing Key Laboratory of Lignocellulosic Chemistry, College of Materials Science and Technology, Beijing Forestry University, Beijing 100083, P. R. China. E-mail: zmxue@bjfu.edu.cn

[b]Department of Chemistry, Renmin University of China, Beijing 100872, P. R. China. E-mail: tcmu@ruc.edu.cn

Materials

5-hydroxymethylfurfural (HMF), 5-hydroxymethyl-2-furancarboxylic acid (HMFCA), 2,5-diformylfuran (DFF), 5-formyl-2-furan-carboxylic acid (FFCA), 2,5-furandicarboxylic acid (FDCA) and ammonium formate were purchased from Innochem Science & Technology Co., Ltd (Beijing, China). Cobalt chloride hexahydrate ($CoCl_2 \cdot 6H_2O$, AR, ≥ 99.5%), nickel (II) chloride hexahydrate ($NiCl_2 \cdot 6H_2O$, AR, ≥ 99.5%), thiourea, polyethylene glycol 200 (PEG200) and potassium hydroxide (KOH, AR, ≥ 99.5%) were received from Aladdin Reagents Co., Ltd (Shanghai, China). All the chemicals were used as received without purification. Nafion was purchased from Shanghai Macklin Biochemical Co., Ltd. The nickel foam (NF) with a purity > 99.99% was purchased from Sheng Qiang Co., Ltd (Jiangsu, China). The NF was cleaned with 3 M hydrochloric acid, ethanol, and deionized water for 10 minutes each before use.

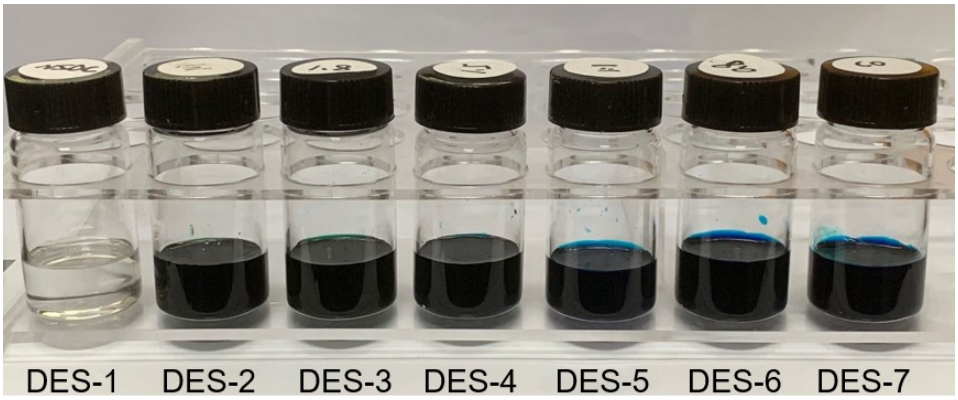

Fig. S1. Schematic diagram of deep eutectic solvents (DESs) with different ratios of nickel and cobalt.

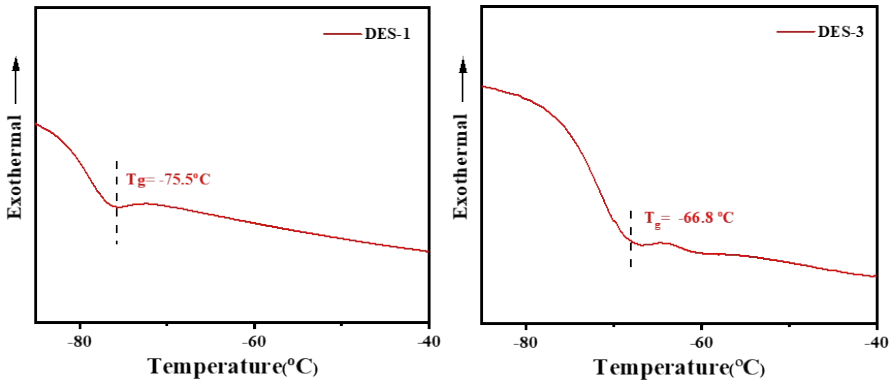

Fig. S2. Differential Scanning Calorimeter (DSC) spectra of deep eutectic solvents of DES-1 and DES-3 (PEG200, T_g = -65 °C; Thiourea, T_g =170 °C; Cobalt chloride hexahydrate, T_g =86 °C; Nickel (II) chloride hexahydrate, T_g = 140 °C).

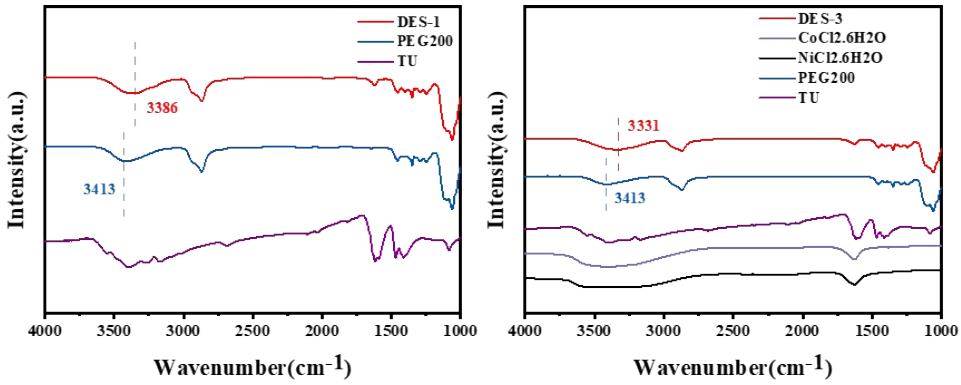

Fig. S3. FT-IR spectra of DES-1, DES-2, TU, PEG 200, $NiCl_2 \cdot 6H_2O$ and $CoCl_2.6H_2O$.

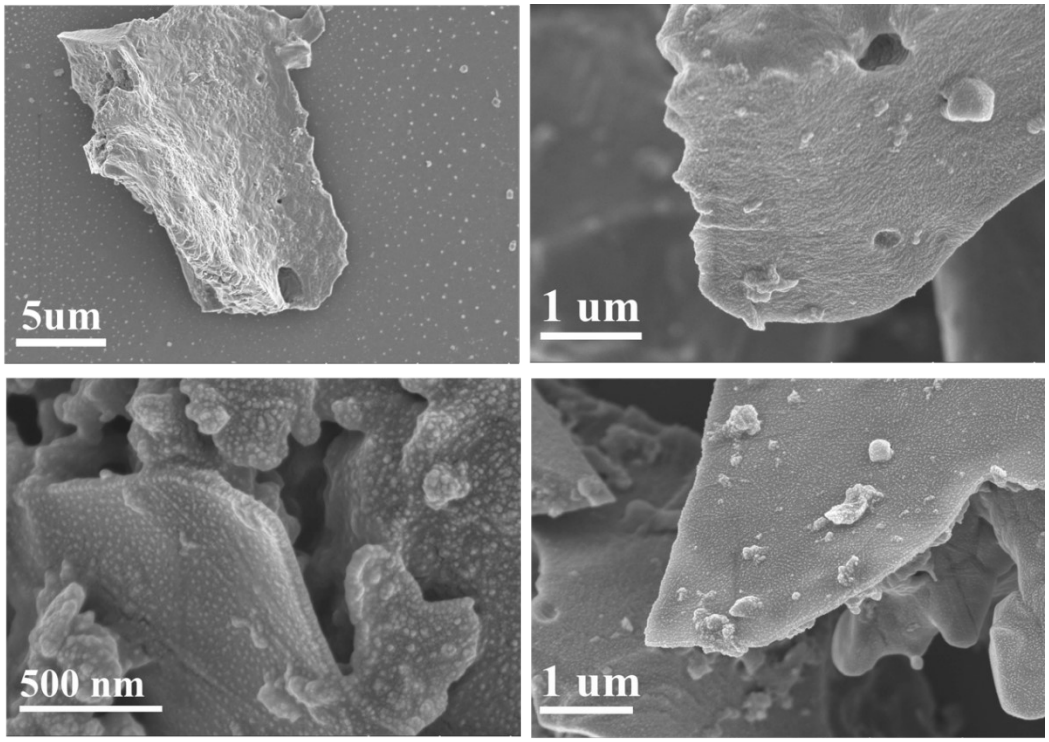

Fig. S4. SEM images of DES-1 after one-step pyrolysis strategy (NSOC).

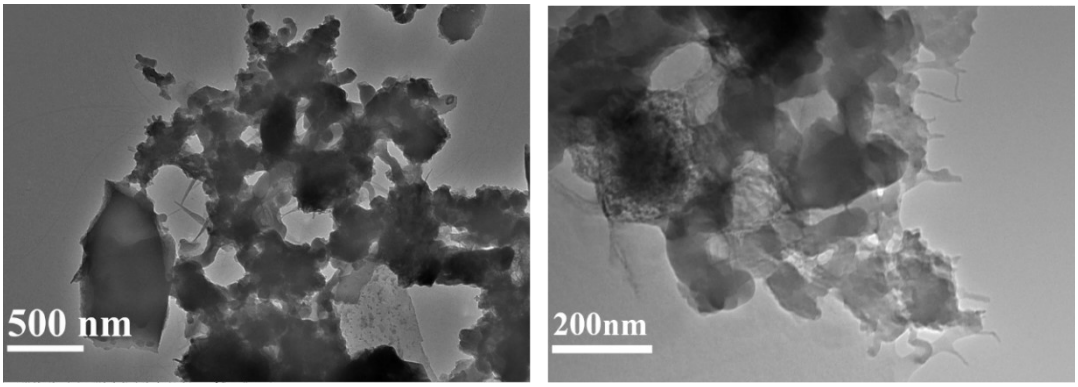

Fig. S5. TEM images of NSOC.

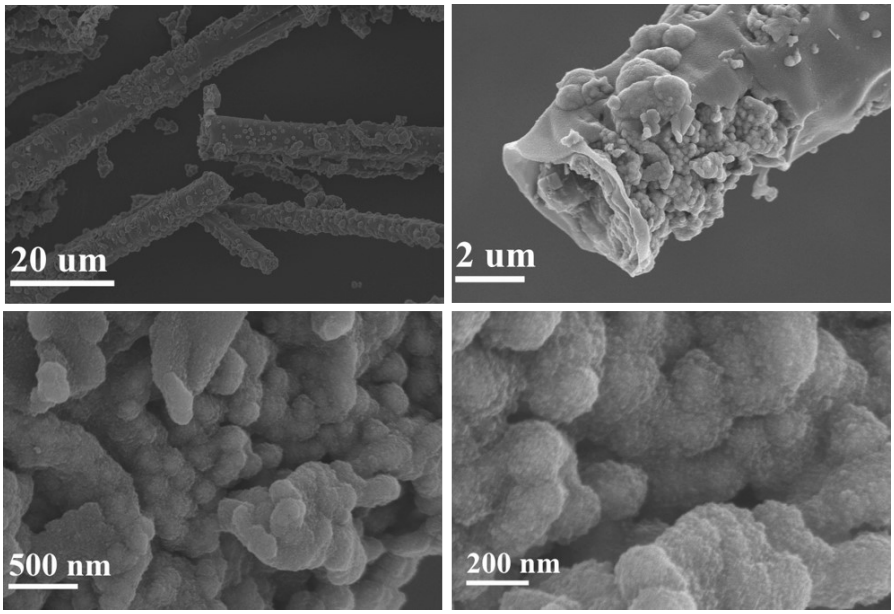

Fig. S6. SEM images of DES-2 after one-step pyrolysis and sulfuration strategy (Ni_3S_2@NSOC).

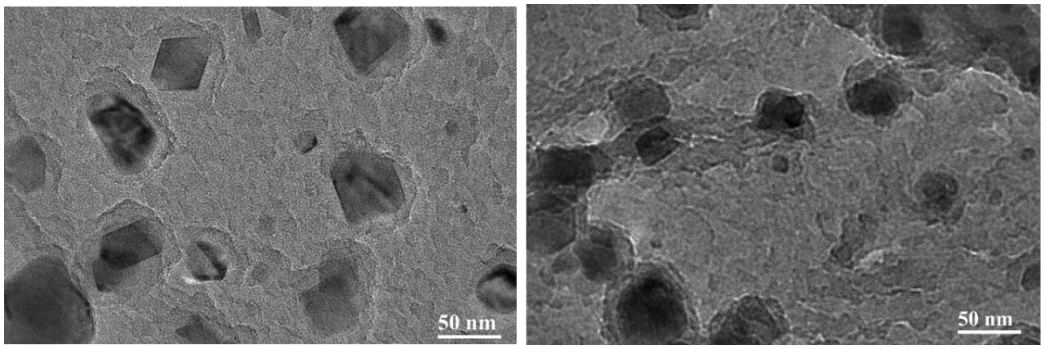

Fig. S7. TEM images of Ni_3S_2@NSOC.

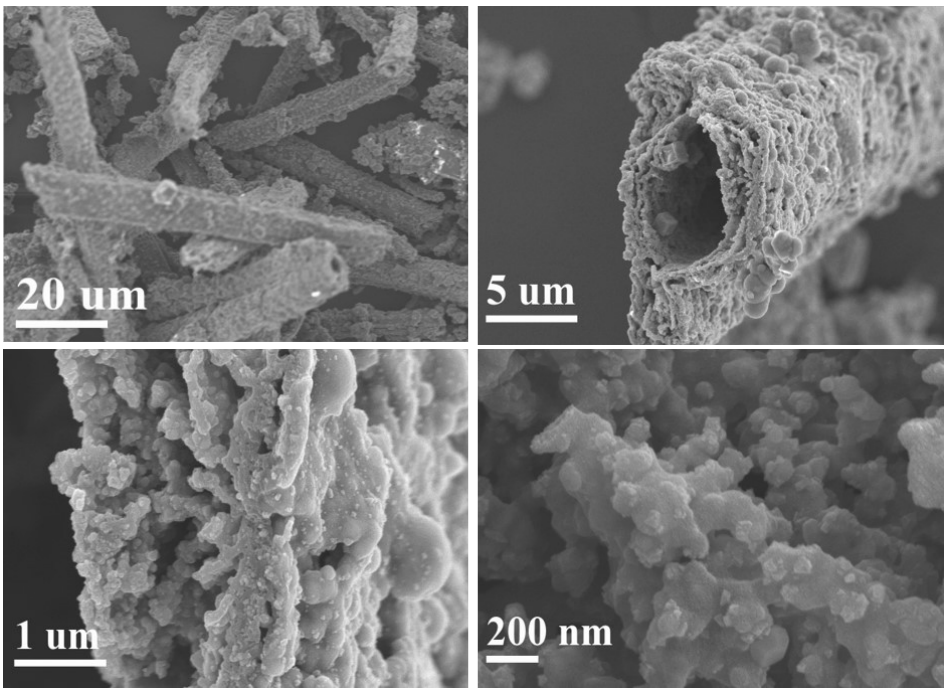

Fig. S8. SEM images of DES-3 after one-step pyrolysis and sulfuration strategy (Co_9S_8-Ni_3S_2@NSOC).

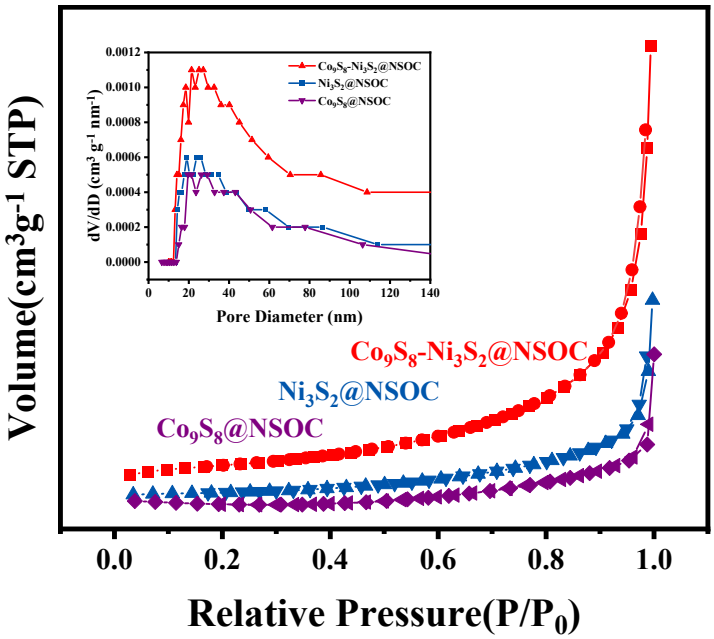

Fig. S9. N_2 adsorption-desorption isotherms (inset: pore size distribution) of Co_9S_8 @NSOC, Ni_3S_2@NSOC, and Co_9S_8-Ni_3S_2@NSOC.

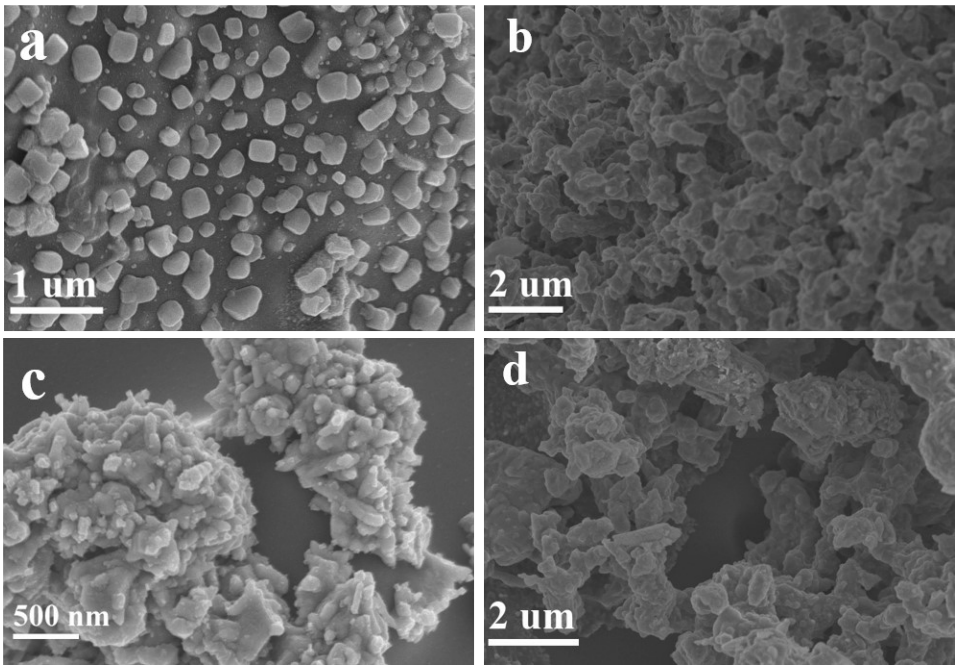

Fig. S10. SEM images of a) DES-4, b) DES-5, c) DES-6, d) DES-7 after one-step pyrolysis and sulfuration strategy.

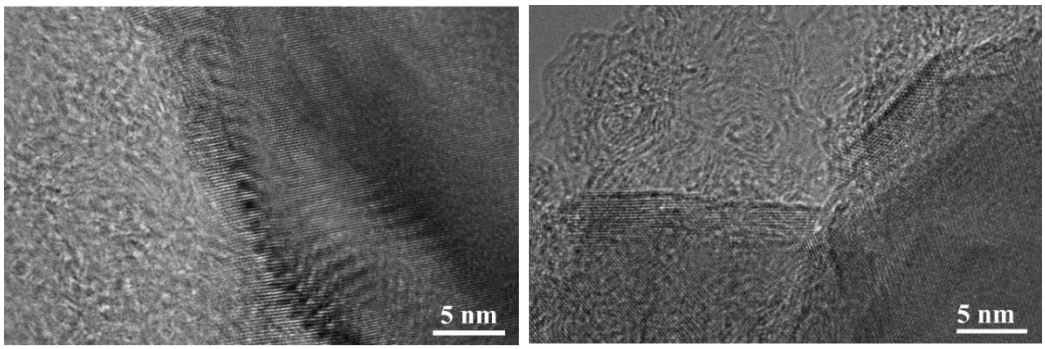

Fig. S11. HRTEM images of Co_9S_8-Ni_3S_2@NSOC.

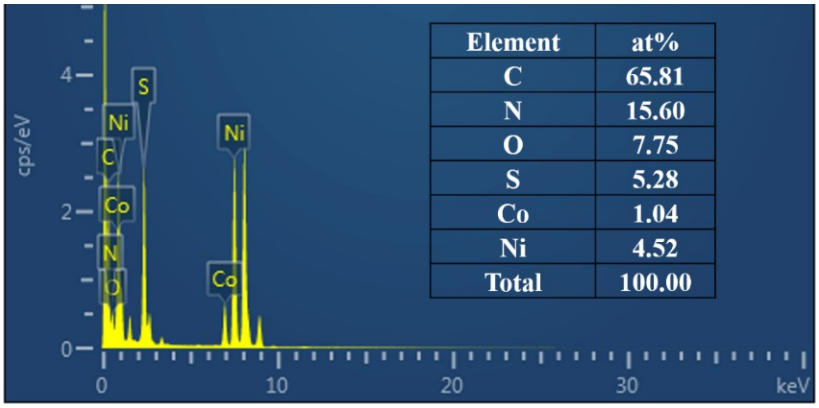

Fig. S12. Energy dispersive spectroscopy (EDS) of Co_9S_8-Ni_3S_2@NSOC.

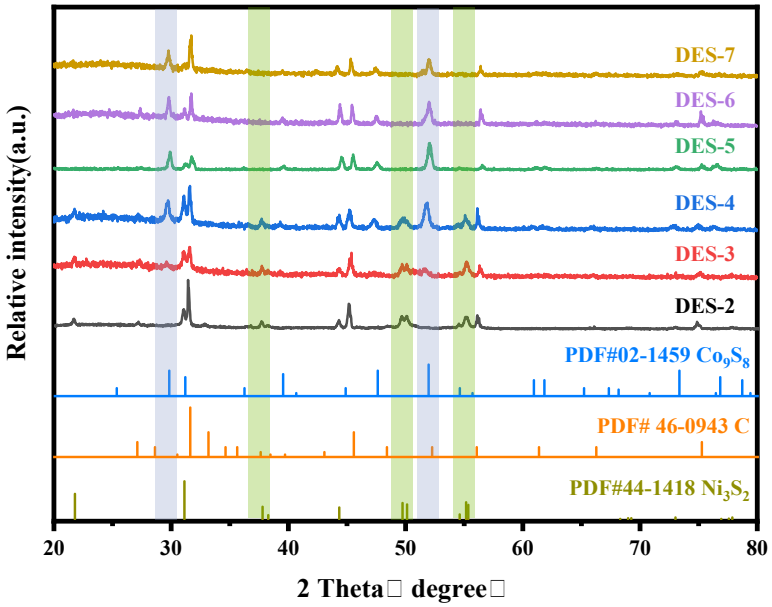

Fig. S13. PXRD patterns of the samples obtained from DES at different molar ratio (DES-2~DES-7 as precursors, 3 h, 400 °C).

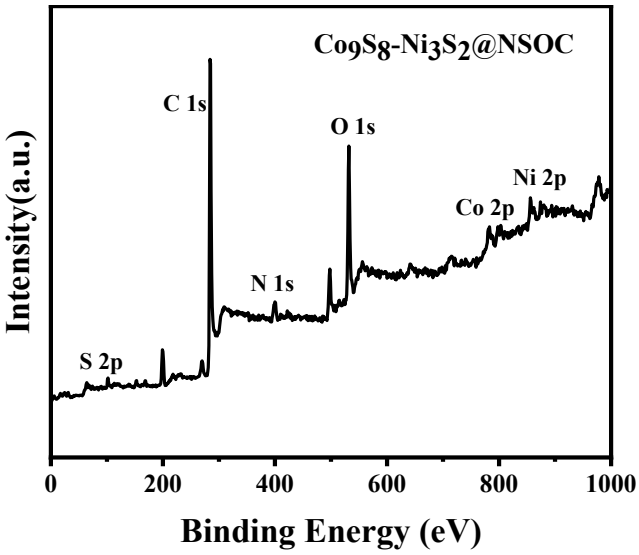

Fig. S14. XPS survey spectrum of Co_9S_8-Ni_3S_2@NSOC hybrid.

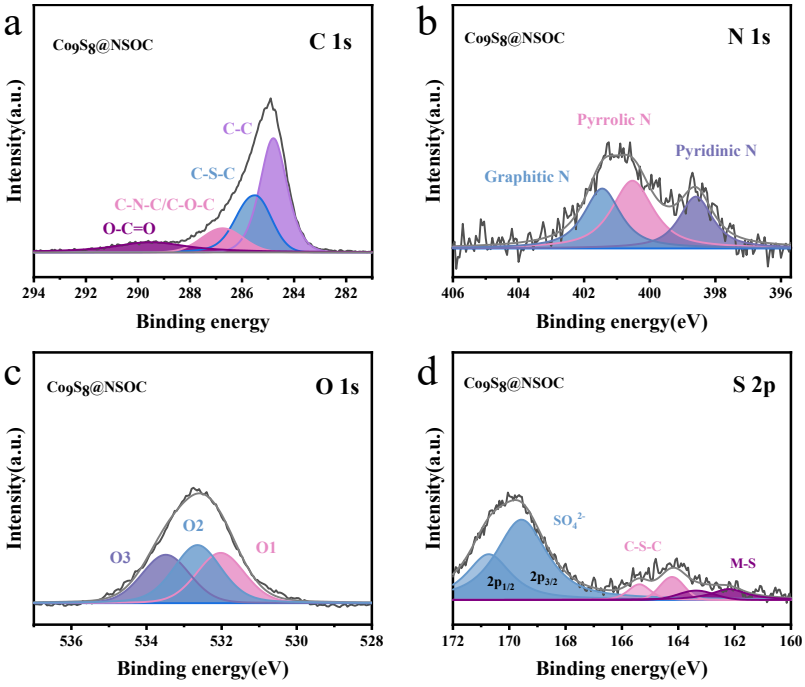

Fig. S15. XPS spectra of (a) C 1s, (b) N 1s , (c) O 1s and (d) S 2p for Co_9S_8@NSOC.

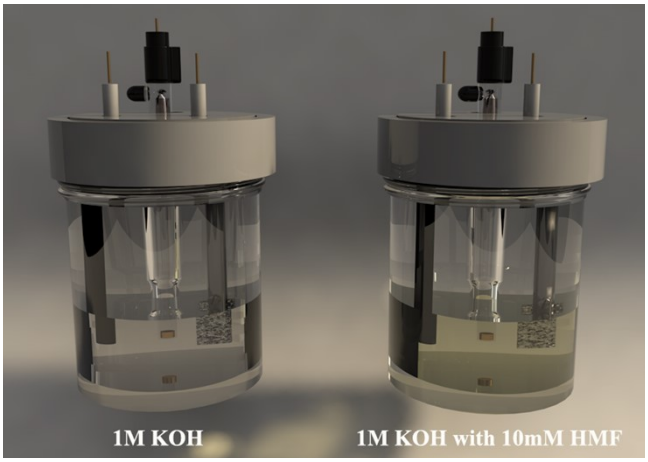

Fig. S16. Typical three-electrode model.

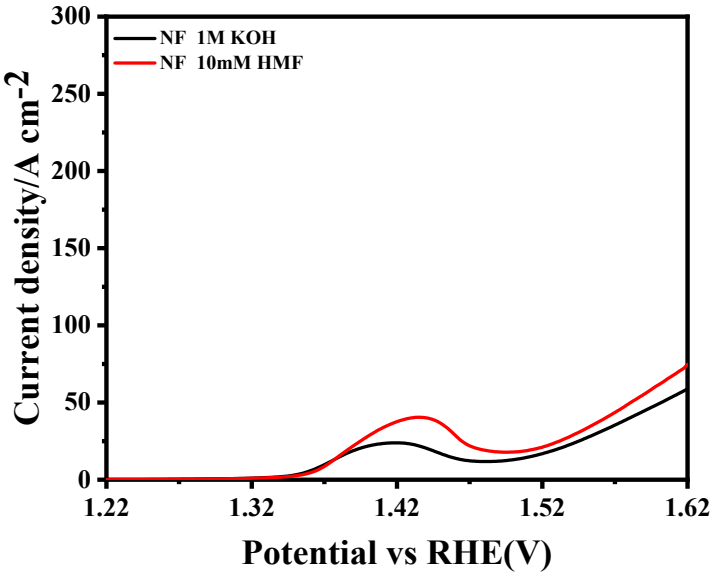

Fig. S17. Polarization curves of NF in 1.0 M KOH and 1.0 M KOH with 10 mM HMF after CV.

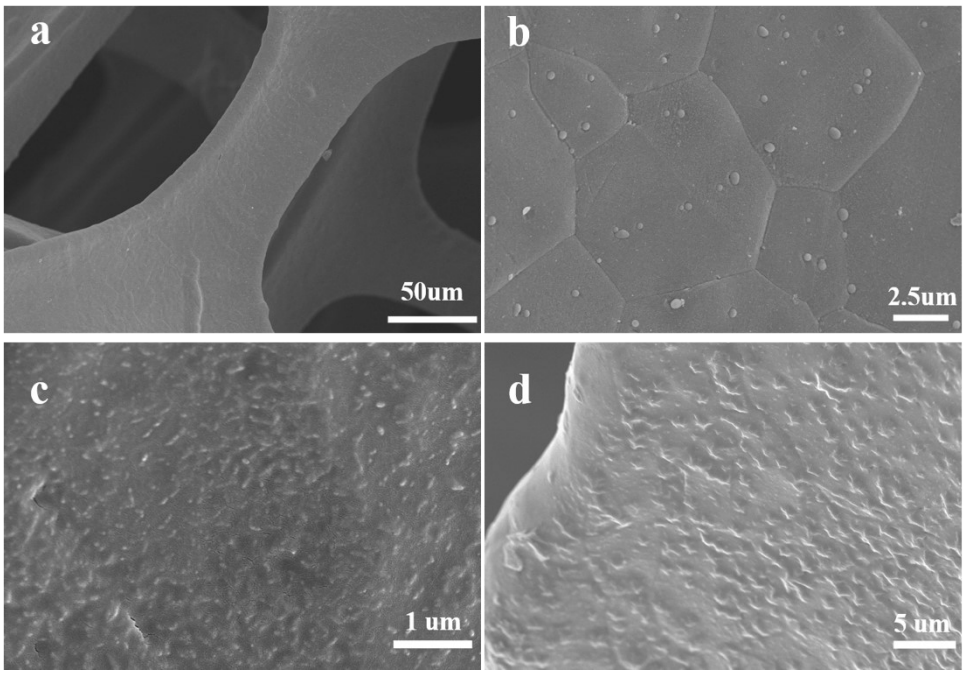

Fig. S18. SEM images of bare NF electrode a, b) before CV activation; c, d) after CV activation.

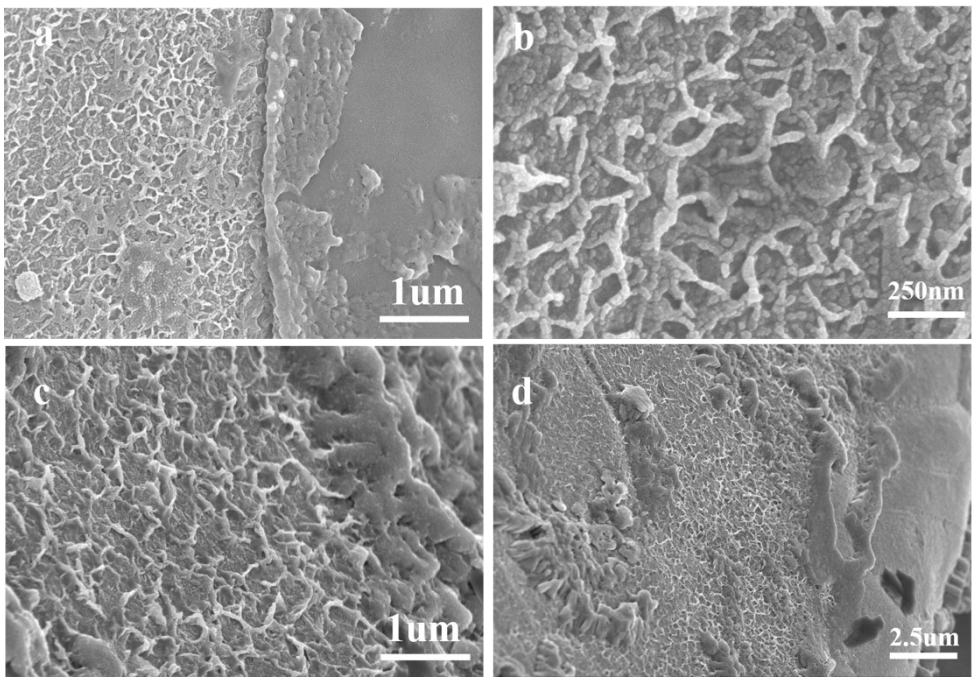

Fig. S19. SEM images of after CV activation. a, b) NSOC/NF electrode; c, d) Ni_3S_2@NSOC/NF electrode.

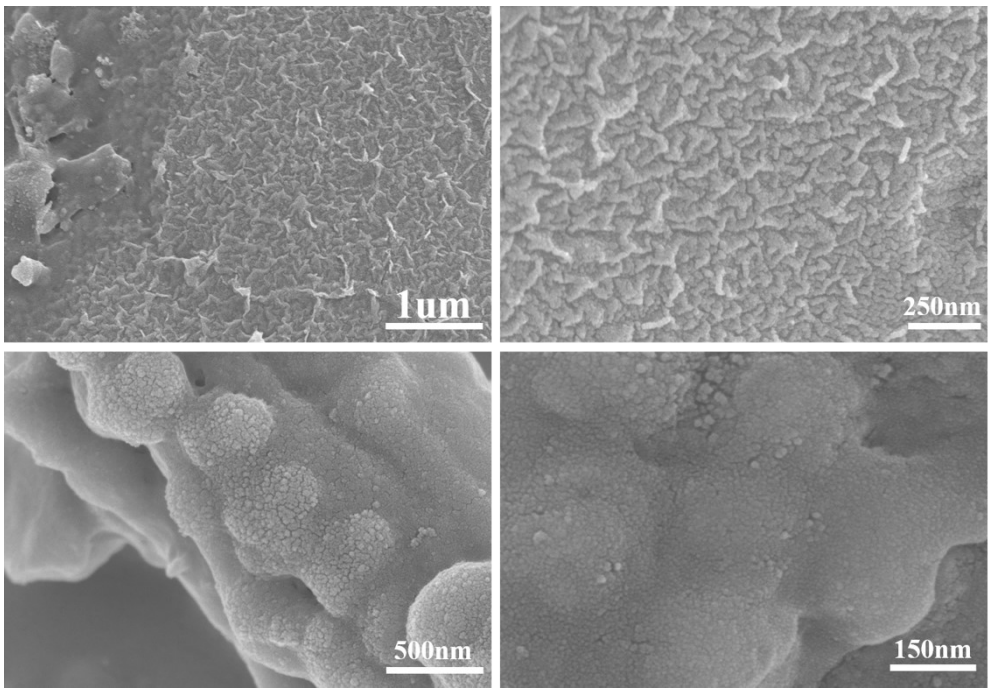

Fig. S20. SEM images of Co_9S_8-Ni_3S_2@NSOC/NF electrode after CV activation.

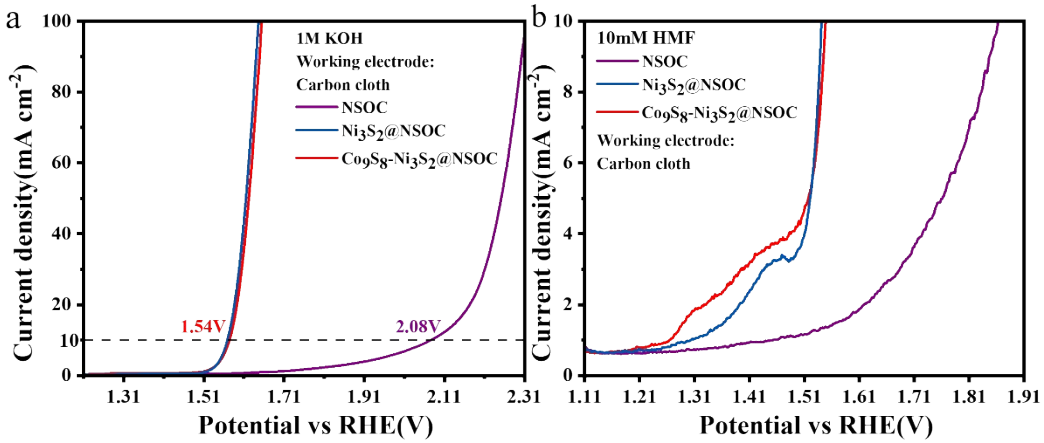

Fig. S21. a) LSV curves for Co_9S_8-Ni_3S_2@NSOC/CC, Ni_3S_2@NSOC/CC and NSOC/CC in 1 M KOH without HMF (10 mM) and b) with10 mM HMF (scan rate, 5 mV s^{-1})

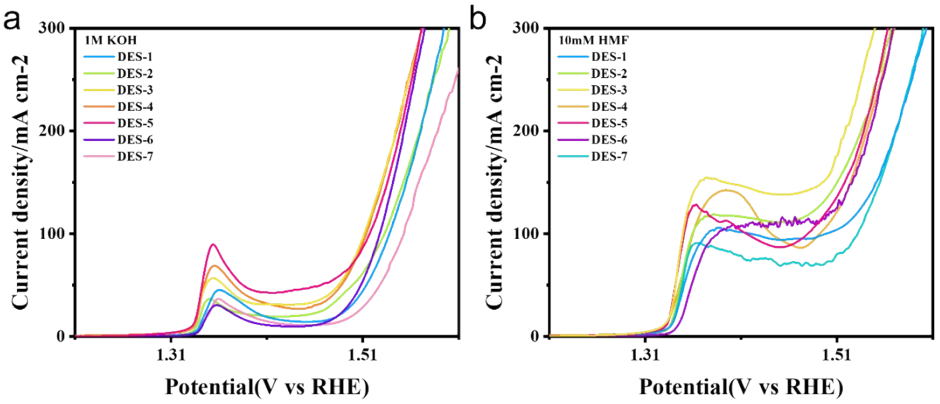

Fig. S22. a) The polarization curves of the samples obtained from DES at different molar ratio (DES-1~DES-7 as precursors, 3 h, 400 ºC) in 1.0M KOH solution, and b) Polarization curves in 1.0 M KOH with 10 mM HMF.

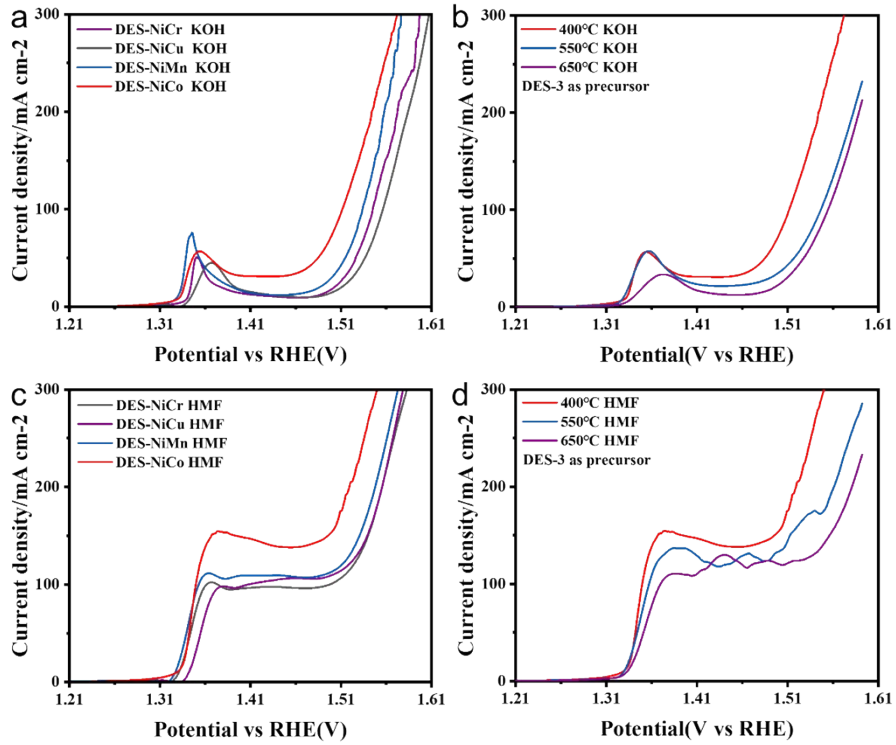

Fig. S23. a, b) The polarization curves of samples obtained from DES at different elements, different pyrolysis temperatures in 1.0 M KOH solution and c, d) Polarization curves in 1.0 M KOH with 10 mM HMF.

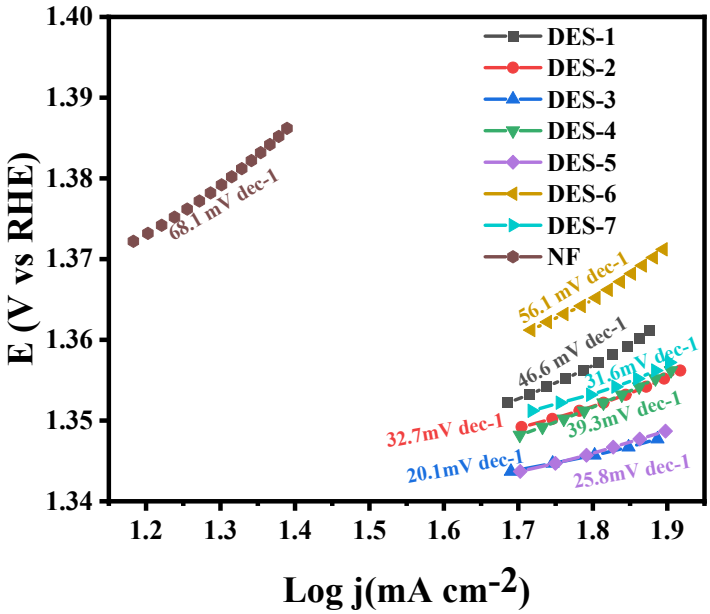

Fig. S24. Tafel slopes of the samples obtained from DES at different molar ratio (DES-1~DES-7 as precursors, 3 h, 400 °C) and bare NF.

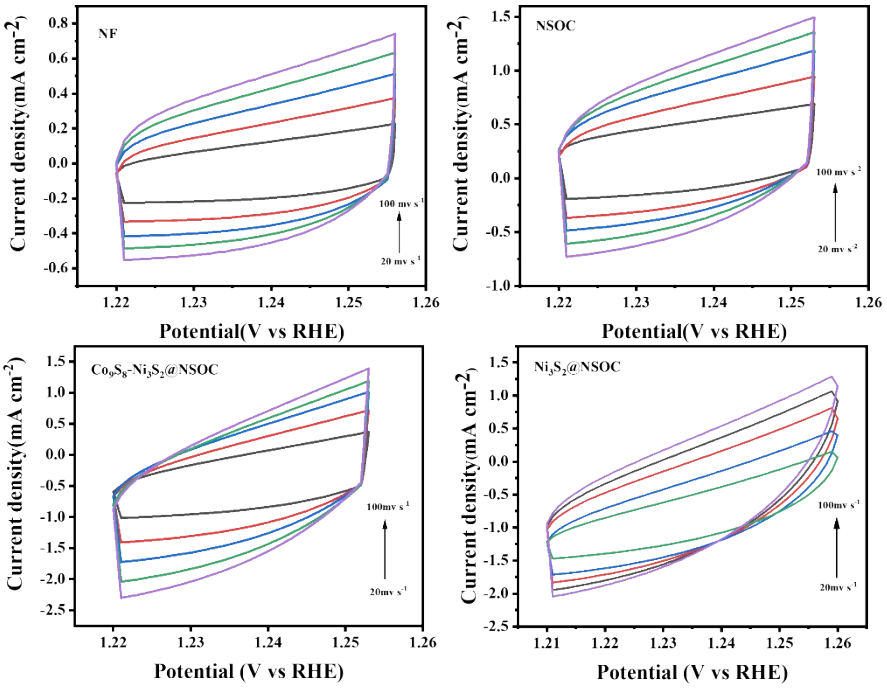

Fig. S25. Cyclic voltammetry of catalysts (1.21-1.26 V vs. RHE) at different scan rate.

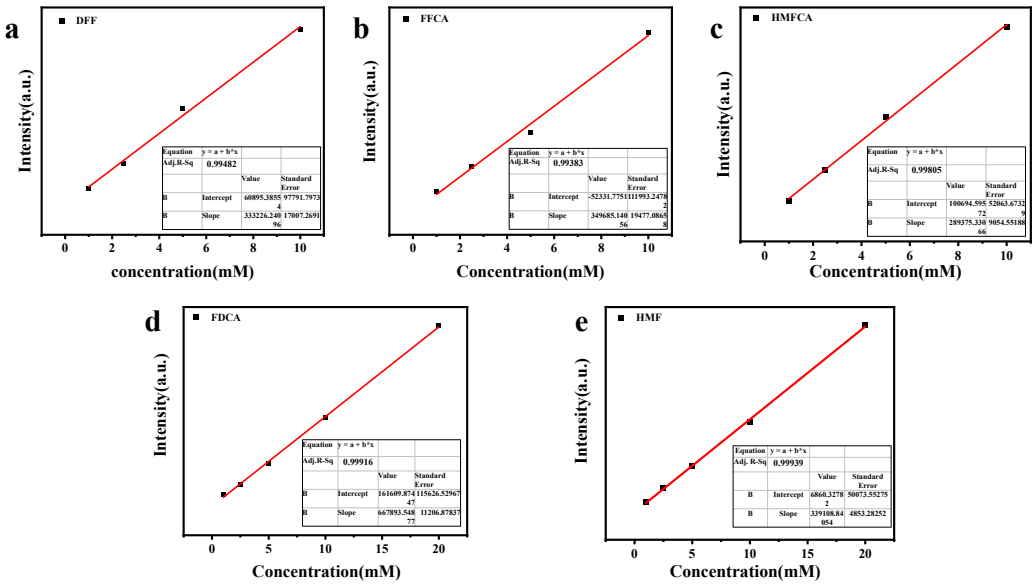

Fig. S26. HPLC standard curve measurements of pure a) DFF, b) FDCA, c) HMFCA, d) FDCA and e) HMF.

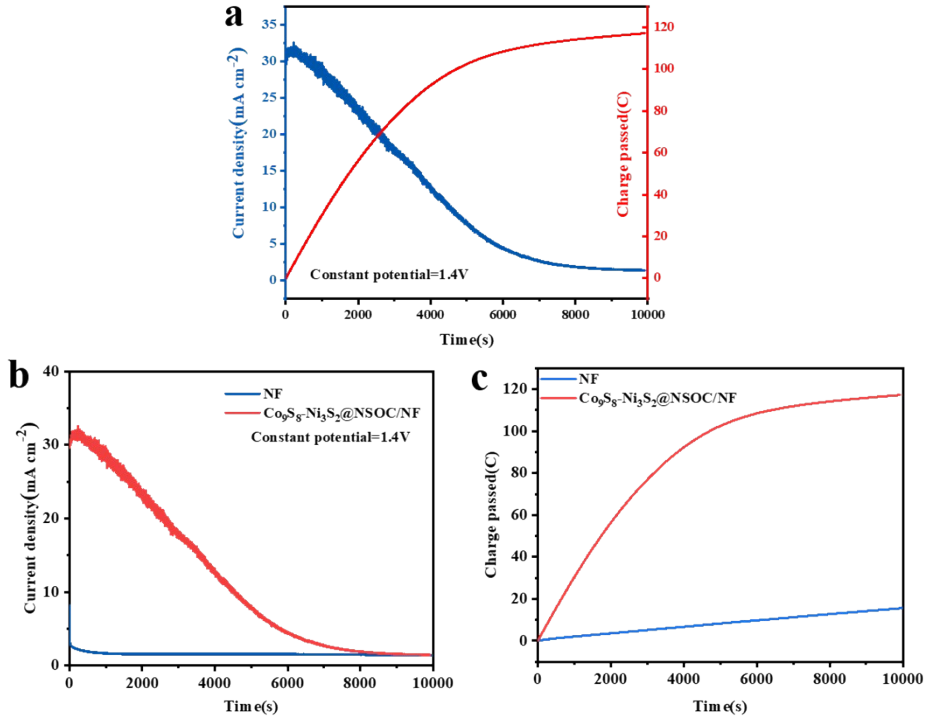

Fig. S27. a) Controlled potential electrolysis of Co_9S_8-Ni_3S_2@NSOC/NF, b) current vs time and c) The comparison of charge vs time for Co_9S_8-Ni_3S_2@NSOC/NF (red) and NF (blue) during the electrolysis at a constant potential of 1.4 V vs RHE in 1 M KOH with the presence of 10 mM HMF.

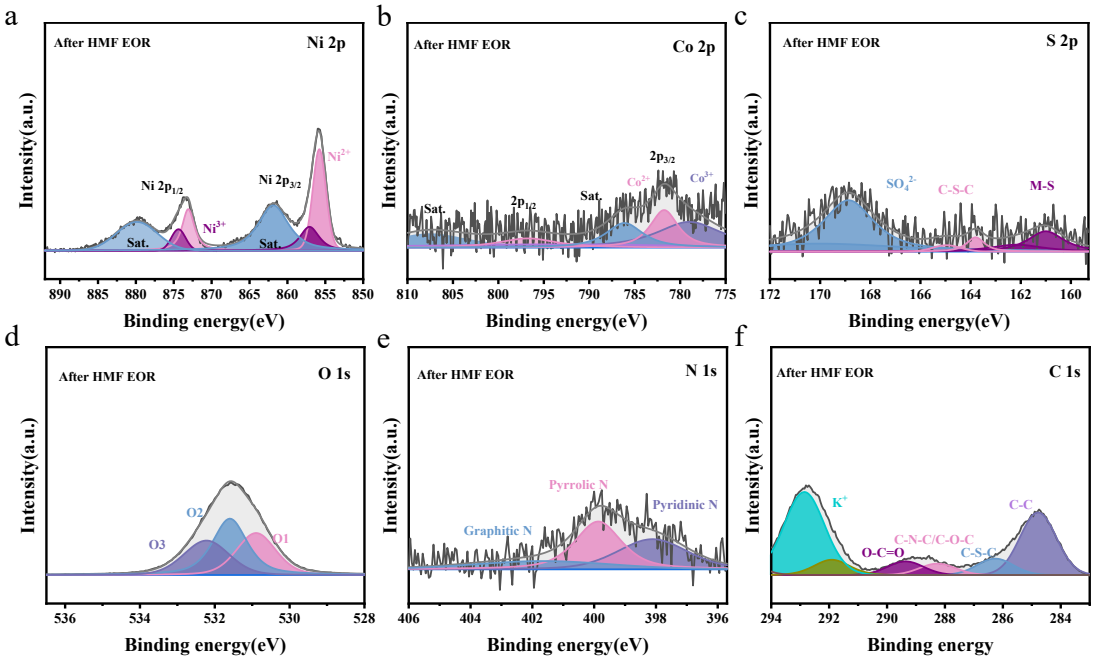

Fig. S28. XPS spectra a) Ni 2p, b) Co 2p, c) S 2p, d) O 1s, e) N 1s and f) C 1s of the Co_9S_8-Ni_3S_2@NSOC/NF after HMF EOR.

Table S1. Relevant reagents, sources of different proportions, and Co sources for the prepared samples.

Sample	PEG200 (g)	$NiCl_2.6H_2O$ (mmol)	$CoCl_2.6H_2O$ (mmol)	Thiourea (mmol)	(400 °C/3 h/N_2) One-step pyrolysis
DES-1	6	0	0	5	NSOC
DES-2	6	5	0	5	Ni_3S_2@NSOC
DES-3	6	4.5	0.5	5	Co_9S_8-Ni_3S_2@NSOC
DES-4	6	3.75	1.25	5	CoS_x-NiS_x@NSOC
DES-5	6	2.5	2.5	5	CoS_x-NiS_x@NSOC
DES-6	6	2	3	5	CoS_x-NiS_x@NSOC
DES-7	6	0	5	5	Co_9S_8@NSOC

Table S2. Elemental analysis results of the catalysts.

Catalysts	N (wt%)	C (wt%)	H (wt%)	S (wt%)	Ni (wt%)	Co (wt%)
NSOC	3.1	74.6	1.3	0.7	---	---
Ni_3S_2@NSOC	2.8	33.8	1.7	12.7	32.4	---
Co_9S_8-Ni_3S_2@NSOC	2.6	30.9	1.4	13.9	29.9	5.9
Co_9S_8@NSOC	3.2	32.3	1.5	14.1	---	31.2

Table S3. The polarization curve potential of the prepared catalyst in 1M KOH or 10 mM HMF on nickel foam（NF）

	OER (V)[a]		HMF EOR (V)[a]			ΔE (mV)[b]	
Precursor	10 mA/cm^2	100 mA/cm^2	10 mA/cm^2	50 mA/cm^2	100 mA/cm^2	10 mA/cm^2	100 mA/cm^2
DES-7	1.343	1.555	1.338	1.352	1.534	5	21
DES-6	1.345	1.530	1.346	1.361	1.389	-1	141
DES-5	1.335	1.520	1.338	1.344	1.353	-3	167
DES-4	1.336	1.517	1.333	1.348	1.363	3	154
DES-3	1.335	1.514	1.330	1.345	1.352	5	162
DES-2	1.343	1.540	1.339	1.353	1.362	4	163
DES-1	1.340	1.535	1.338	1.349	1.377	2	173
NF	1.363	1.690	1.365	1.573	1.651	-2	39.0

[a)](V) are the potentials at 10 and 100 mA cm^{-2}, respectively, recorded under stirring at room temperature with 90% iR-correction. [b)]ΔE represents the difference between KOH and HMF.

Table S4. The HMF EOR performance of the different catalysts.

Performance Catalysts	Parameters	NSOC /NF	Ni_3S_2@NSOC /NF	Co_9S_8-Ni_3S_2@NSOC /NF
HMF EOR	η10, η100 (V)	1.338, 1.377	1.339, 1.362	1.330, 1.352
	Tafel slopes (mV dec^{-1})	46.6	32.7	20.1
	Conversion (%)	90.4	94.8	99.5
	Selectivity (%)	87	90.7	98.8
	FE (%)	86.8	90.5	98.6

Table S5. The comparison of activity for Co_9S_8-Ni_3S_2@NSOC and other reported catalysts.

Electrode Materials	Electrolysis potential	FDCA yield	Faradaic efficiency	Catalyst loading	Catalyst substrate	Ref.
Co_9S_8-Ni_3S_2@NSOC	1.40 V	98.8%	98.6%	0.3 mg.cm^{-2}	Nickel foam	This work
NSOC	1.40 V	87%	86.8%	0.3 mg.cm^{-2}	Nickel foam	This work
BNC-2	1.90 V	57%	---	0.3 mg.cm^{-2}	carbon paper	[1]
S-Ni@C	1.473 V	96%	96%	3.0 mg.cm^{-2}	carbon paper	[2]
MoO_2-FeP@C	1.424 V	98%	97.8%	1.9 mg.cm^{-2}	Nickel foam	[3]
P-HEOs	1.50 V	97.4%	96.6%	0.8 mg.cm^{-2}	carbon paper	[4]
$Ni_{0.9}Cu_{0.1}(OH)_2$	1.45 V	91.2%	91.2%	1.0 mg.cm^{-2}	carbon paper	[5]
NiBx@NF	1.64 V	99%	99.5%	2.47 mg.cm^{-2}	Nickel foam	[6]
$CuCo_2O_4$	1.45 V	93.70%	94%	---	Nickel foam	[7]
Ni_3S_2/NF	1.423 V	100%	98%	---	Nickel foam	[8]
Ni_2P/NF	1.423 V	100%	~100 %	---	Nickel foam	[9]
CoFe@NiFe	1.40V	100%	99.8%	---	Nickel foam	[10]
$NiCo_2O_4$	1.43V	90.80%	87.50%	---	Nickel foam	[11]
NiSe@NiO_x	1.423V	~99%	~99%	---	Nickel foam	[12]
Co_3O_4 NW/NF	1.469V	96.8%	95.9%	---	Nickel foam	[13]
CoNiFe LDH	1.55V	84.9%	~90%	---	Carbon fiber paper	[14]

References

1. Q. Qin, T. Heil, J. Schmidt, M. Schmallegger, G. Gescheidt, M. Antonietti and M. Oschatz, *Applied Energy Materials*, 2019, **2**, 8359-8365.
2. F. Kong and M. Wang, *ACS Appl. Energy Mater.*, 2021, **4**, 1182-1188.
3. G. Yang, Y. Jiao, H. Yan, Y. Xie, A. Wu, X. Dong, D. Guo, C. Tian and H. Fu, *Adv. Mater.*, 2020, **32**, 2000455.
4. K. Gu, D. Wang, C. Xie, T. Wang, G. Huang, Y. Liu, Y. Zou, L. Tao and S. Wang, *Angew. Chem. Int. Ed.*, 2021, **60**, 20253-20258.
5. J. Zhang, P. Yu, G. Zeng, F. Bao, Y. Yuan and H. Huang, *J. Mater. Chem. A*, 2021, **9**, 9685-9691.
6. P. Zhang, X. Sheng, X. Chen, Z. Fang, J. Jiang, M. Wang, F. Li, L. Fan, Y. Ren, B. Zhang, B. J. J. Timmer, M. S. G. Ahlquist and L. Sun, *Angew. Chem. Int. Ed.*, 2019, **58**, 9155-9159.
7. Y. Lu, C.-L. Dong, Y.-C. Huang, Y. Zou, Z. Liu, Y. Liu, Y. Li, N. He, J. Shi and S. Wang, *Angew. Chem. Int. Ed.*, 2020, **59**, 19215-19221.
8. B. You, X. Liu, N. Jiang and Y. Sun, *J. Am. Chem. Soc.*, 2016, **138**, 13639-13646.
9. B. You, N. Jiang, X. Liu and Y. Sun, *Angew. Chem. Int. Ed.*, 2016, **55**, 9913-9917.
10. Y. Xie, Z. Zhou, N. Yang and G. Zhao, *Adv. Funct. Mater.*, 2021, **31**, 2102886.
11. M. J. Kang, H. Park, J. Jegal, S. Y. Hwang, Y. S. Kang and H. G. Cha, *Appl. Catal. B*, 2019, **242**, 85-91.
12. L. Gao, Z. Liu, J. Ma, L. Zhong, Z. Song, J. Xu, S. Gan, D. Han and L. Niu, *Appl. Catal. B*, 2020, **261**, 118235.
13. Z. Zhou, C. Chen, M. Gao, B. Xia and J. Zhang, *Green Chem.*, 2019, **21**, 6699-6706.
14. M. Zhang, Y. Liu, B. Liu, Z. Chen, H. Xu and K. Yan, *ACS Catal.*, 2020, **10**, 5179-5189.